

AD-A134-416

SPECIES-SPECIFIC DENSITIES OF STATES OF GA AND AS IN  
THE CHEMISORPTION OF OXYGEN ON GAAS(110)(U) WISCONSIN  
UNIV-MADISON K D CHILDS ET AL. 15 SEP 83 TR-9

1/1

UNCLASSIFIED

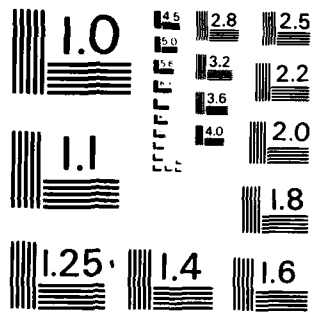
N00014-77-C-0474

F/G 20/12

NL



END  
DATE  
FILMED  
91-03  
DTIC



MICROCOPY RESOLUTION TEST CHART  
NATIONAL BUREAU OF STANDARDS - 1963 - A

REPORT DOCUMENTATION PAGE		READ INSTRUCTIONS BEFORE COMPLETING FORM
1. REPORT NUMBER N00014-77-C-0474-9	2. GOVT ACCESSION NO.	3. RECIPIENT'S CATALOG NUMBER
4. TITLE (and Subtitle) SPECIES-SPECIFIC DENSITIES OF STATES OF Ga AND As IN THE CHEMISORPTION OF OXYGEN ON GaAs(110)		5. TYPE OF REPORT & PERIOD COVERED Technical Report
7. AUTHOR(s) K. D. Childs and M. G. Lagally		6. PERFORMING ORG. REPORT NUMBER
9. PERFORMING ORGANIZATION NAME AND ADDRESS Board of Regents of the University of Wisconsin System, 750 University Ave., Madison, WI 53706		8. CONTRACT OR GRANT NUMBER(s) N00014-77-C-0474
11. CONTROLLING OFFICE NAME AND ADDRESS Office of Naval Research Arlington, VA 22217		10. PROGRAM ELEMENT, PROJECT, TASK AREA & WORK UNIT NUMBERS NR 322-072
14. MONITORING AGENCY NAME & ADDRESS (if different from Controlling Office) Office of Naval Research Branch Office Chicago 536 S. Clark Street, Room 286 Chicago, IL 60605		12. REPORT DATE September 15, 1983
16. DISTRIBUTION STATEMENT (of this Report) Approved for public release; distribution unlimited.		13. NUMBER OF PAGES 36
17. DISTRIBUTION STATEMENT (of the abstract entered in Block 20, if different from Report)		14. SECURITY CLASS. (of this report) Unclassified
18. SUPPLEMENTARY NOTES Submitted to Physical Review		15a. DECLASSIFICATION/DOWNGRADING SCHEDULE
19. KEY WORDS (Continue on reverse side if necessary and identify by block number) Surfaces, semiconductors, GaAs(110), local electronic properties, Auger line shapes, oxygen chemisorption.		
20. ABSTRACT (Continue on reverse side if necessary and identify by block number) Auger line shape measurements have been made to extract the variation in the local charge distribution around Ga and As sites for chemisorption of oxygen on cleaved and sputter-etched GaAs(110). A significant variation with changing O coverage is observed in the Ga spectrum, with a much more subtle change in the As spectrum. Conclusions on the nature of the bonding and on the mechanism for adsorption at both low and high coverages are drawn from these spectra.		

AD-A234476

DTIC FILE COPY

DTIC  
ELECTE  
NOV 2 1983  
S D D

Accession For	
NTIS GRA&I	<input checked="" type="checkbox"/>
DTIC TAB	<input type="checkbox"/>
Unannounced	<input type="checkbox"/>
Justification	
By _____	
Distribution/	
Availability	_____
Dist	_____
A/11	



OFFICE OF NAVAL RESEARCH  
 Contract No. N00014-77-C-0474  
 Project No. 322-072  
 TECHNICAL REPORT-9

SPECIES-SPECIFIC DENSITIES OF STATES OF Ga AND As  
 IN THE CHEMISORPTION OF OXYGEN ON GaAs(110)

by

K. D. Childs and M. G. Lagally  
 Department of Metallurgical and Mineral Engineering  
 and the Materials Science Center  
 University of Wisconsin  
 Madison, Wisconsin 53706

September 15, 1983

Reproduction in whole or in part is permitted  
 for any purpose of the United States Government

DISTRIBUTION OF THIS DOCUMENT IS UNLIMITED

SPECIES-SPECIFIC DENSITIES OF STATES OF  $G_2$  AND AS IN THE  
CIRCUMSCRIPTION OF OXYGEN ON  $G_2As(110)$ \*

K. D. Childs and M. G. Lagally

Department of Metallurgical and Mineral Engineering  
and Materials Science Center  
University of Wisconsin  
Madison, Wisconsin 53706

\*Research Supported by UNH

#### Abstract

Auger line shape measurements have been made to extract the variation in the local charge distribution around W and As sites for chemisorption of oxygen on cleaved and sputter-etched WAs(110). A significant variation with changing O coverage is observed in the W spectrum, with a much more subtle change in the As spectrum. Conclusions on the nature of the bonding and on the mechanism for adsorption at both low and high coverages are drawn from these spectra.

#### 1. INTRODUCTION

Because of the possible technological importance of oxides on III-V compounds, the adsorption of oxygen on WAs surfaces has been extensively investigated. In particular the adsorption site and the nature of the chemical interaction between O and the W or As atoms on WAs(110) has generated considerable experimental and theoretical effort. The results of these studies can be summarized as follows. It is generally believed on the basis of electron energy loss spectroscopy, low-energy electron diffraction, and x-ray or ultraviolet photoelectron spectroscopy that both W and As atoms in WAs(110) participate in bonding to O. (1-6) Two adsorption regimes appear to exist, with a dividing line roughly at a coverage of  $\theta = 0.05$  to  $0.1$ . (4,5) If a molecularly adsorbed state exists at all it exists only below this coverage, i.e., the chemisorption of O is dissociative over most and possibly all of the coverage range. (1-8) Defects on the surface appear to be important both in providing initial adsorption sites and in the dissociation of  $O_2$  molecules, causing the chemisorption of atomic oxygen even if care is taken to avoid atomic oxygen in the exposure. (4-8) Atomic oxygen is adsorbed at a much faster rate than is molecular oxygen. (1,8,11) A surface with a high defect density adsorbs oxygen faster than one with a low density. (3,9,12) These conclusions are in the main drawn on the basis of core-level chemical shifts and changes in valence band photoemission and electron energy loss spectra as a function of O exposure, with some supporting evidence from LEIS measurements. A number of models for the adsorption site and the resultant "surface molecule" have been proposed, including O bridge bonds between W and As surface atoms, (2) separate W-O and As-O bonds, (5) surface oxides, (4) and more complex arrangements. (13) Theoretical results indicate, however, that it may not be straightforward to draw conclusions

about the bonding sites simply from chemical shifts in the behavior of energy loss peaks, because adsorption on one kind of site (e.g., As) may cause charge transfer between species, thus affecting the charge distribution around those species. As a consequence, the interpretation of spectroscopic results may be misleading. (10,11,14-18) In some of these calculations (17) it is possible to project out the local density of states at each species as a function of the bonding geometry of the adsorbate and to follow changes in this local density of states as a function of coverage. When compared to such calculations, a measurement of the local, or species-specific, valence band density of states may aid in determining the bonding site and the local chemical changes that occur upon chemisorption. Such a measurement is possible by observing for each species of interest an Auger transition that involves the valence band, because of the dipole-dipole nature of the Auger process, the probability of finding the "up" electron in an Auger transition a distance  $R$  from the initial core hole falls off as  $1/R^6$ , and the integrated Auger current as  $1/R^4$ . (19) In particular, core-core-valence Auger transitions are readily related to a species-specific valence band density of states. (20,21) The species specificity of the Auger process has been demonstrated experimentally for a number of materials (20-23) and a comparison between experimental and theoretical (20) results has been made for clean GaAs(110). (21) Here we report on measurements of core-core-valence Auger transitions of Ga and As as a function of oxygen exposure at room temperature for both cleaved GaAs(110) and GaAs(110) that has been damaged by sputter etching. We extract from these measurements Auger lineshapes that can be interpreted as a fingerprint of the species-specific density of states around the Ga and As sites, and follow changes in these lines with oxygen coverage.

## 11. EXPERIMENTAL

The experiments were conducted in an ion-pumped UHV system with a base pressure of less than  $1 \times 10^{-10}$  torr on n-type, Te-doped GaAs crystals. (24) Samples were cleaved in vacuum, employing a knife edge and anvil technique that yielded mirror-like (110) surfaces with very few macroscopic striations and a step density, measured independently by LEIS, (25) of less than one step in 60 lattice constants (the instrumental resolution) in any direction on the crystal surface. The disordered surface was prepared by sputter-etching the cleaved surface. No LEIS pattern is observable after this sputter-etching. Auger lines were measured with a single-pass cylindrical mirror analyzer using 2 eV modulation and phase detection for differentiation of the Auger signal. Possible electron beam effects were carefully monitored by making measurements at different doses and comparing these. (26) The Ga and As  $M_{2,3}V$  lines were signal averaged for periods between 10 and 20 minutes, providing a signal-to-noise ratio of approximately 10. These Auger transitions occur at kinetic energies close to the minimum of the electron mean free path, providing very good surface sensitivity. A backscattered-electron spectrum was taken at a primary-beam energy such that the elastically scattered electron peak occurs at the same energy as the Auger data. This backscattered-electron spectrum serves to represent the electron-energy-loss and instrument broadening functions. (27-29) The backscattered-electron spectrum was deconvoluted from the data using the van Cittert iterative deconvolution method. (30) Additionally, Lorentzian functions representative of the two core levels involved in the CLV transitions under investigation were deconvoluted from the data to eliminate core level broadening from the Auger lineshapes. The widths of these Lorentzians were determined by independently measuring the relevant core level widths using XPS. (31) The

function was finally corrected for the changing energy resolution of the analyzer over the energy range of the Auger line. The result is the Auger transition species-specific valence band density of states. This procedure has been discussed in detail elsewhere. (32)

The cleaved and sputter-etched surfaces were exposed to doses from 10 Langmuirs to  $10^{13}$  Langmuirs of oxygen. All oxygen exposures, rather than being cumulative, were made on freshly cleaved or freshly sputter-etched surfaces. Exposures up to  $10^5$  L were made with continuously flowing  $O_2$  from an oxygen permeation tube at pressures between  $10^{-8}$  and  $10^{-4}$  torr for times varying between 15 and 25 minutes. The  $10^6$ ,  $3 \times 10^{11}$ , and  $10^{13}$  L exposures were made by filling the chamber, for each exposure, with oxygen from a fresh one-liter bottle of research-purity oxygen, and exposing the sample for different amounts of time. For all exposures up to  $10^6$  L the pressure was continuously measured with a nude ion gauge. Although the sample surface was not in direct line of sight with the ion gauge, no effort was made to prevent excited or atomic oxygen formation. For the  $3 \times 10^{11}$  L and  $10^{13}$  L exposures the pressures were calculated from the ratio of the volumes of the 1 liter oxygen bottle and the vacuum chamber. These pressures may be uncertain by a factor of 2. Before any Auger data were taken, the chamber was pumped into the  $10^{-9}$  torr range.

Special attention was paid to the influence of  $H_2O$  on the adsorption.  $H_2O$  adsorbs more rapidly than  $O_2$  or  $O$ , (33) and thus it is important to know the fraction of  $H_2O$  in the ambient gas. For  $O_2$  pressures below  $10^{-6}$  torr the  $H_2O$  partial pressure was always less than  $10^{-2}$  times the pressure of  $O_2$ . At higher  $O_2$  pressures the partial pressure of  $H_2O$  was less than  $10^{-3}$  that of

$O_2$ . With the use of a liquid-nitrogen cold finger, the partial pressure of  $H_2O$  was reduced by another factor of 10 to 100. At these partial pressures, the influence of  $H_2O$  on the adsorption of O was negligible.

### III. CHARACTERIZATION OF OXYGEN ON CLEAVED $WAs(110)$

Auger lineshapes for W and As atoms in the cleaved surface have previously been made (21) and compared to calculations. (20) Figure 1 shows the species-specific densities of states for W and As derived from the  $M_{45}V$  transitions. The W and As  $M_{45}V$  lines occur respectively between 115 and 135 eV and between 135 and 160 eV. Spectra 1) and 2) are the lineshapes resulting from the use of two extreme conditions in the deconvolution routine on one set of data. Spectra 2) through 6) are results for four cleaves and for two locations on one cleavage face. In test for the influence of the 2eV modulation on the spectra, spectrum 7) shows data taken with 1 eV modulation. A comparison of all of these spectra demonstrates that the data are reproducible from one sample to the next and that minimal distortion is introduced by varying parameters in the deconvolution procedure within physically reasonable limits. In addition to the kinetic-energy scale, an energy scale referenced to the valence band edge is shown in Fig. 1. This was determined by rigidly aligning (21) the experimental profiles with the theoretical curves. (20) The resulting peak energies agree very well with those determined by UPS. (21) Although, as has been observed for all other Auger shapes (21,32) a broadening of the line occurs. The W-specific density of states consists of three peaks. Peak "A" at the top of the W-specific density of states is p-like, the middle feature "B" at -6 eV is s-like, and the lower feature "C" at -11 eV is of mixed character. (20) The As-specific density of states consists of three regions; peak "D" at the top of the As



Figure 3 shows the  $M_{45V}$ -derived  $\omega$  and  $\text{As}$  species-specific densities of states for different oxygen coverages on the cleaved surface. The curves are normalized so that the sum of the areas under the  $\omega$  and  $\text{As}$  lines remains constant at different coverages. The  $\omega$ -specific density of states undergoes dramatic changes with increasing coverage. Changes relative to the spectrum for the clean surface are already evident at the lowest coverage at which measurements were made,  $\nu = 0.04$ , with peaks A and C increasing in intensity and peak B broadening. The  $\omega$  spectrum changes insignificantly for coverages between  $\nu = 0.04$  and  $0.12$ . At  $\nu = 0.65$ , intensity at the bottom of the  $\omega$  spectrum which had already begun to increase at  $\nu = 0.3$ , has become a resolvable peak that is shifted by 1.5 eV to a lower binding energy relative to peak C. With increasing coverage this peak continues to increase in intensity, until at 1 monolayer it is as strong as peak B.

The changes in the  $\text{As}$ -specific density of states with changing  $\nu$  coverage are small compared to those for  $\omega$ . These changes appear to be continuous from the lowest coverage up to one monolayer, unlike the changes in the  $\omega$  line, which were dramatic and then became continuous above  $\nu = 0.1$ . The intensity of peak D at the high-energy end of the  $\text{As}$  line decreases, with a corresponding increase at E in the middle of the spectrum.

IV. CHARACTERIZATION OF OXYGEN ON SPUTTER-ETCHED  $\omega\text{As}(110)$

Chemisorption experiments were also performed on sputter-etched surfaces. Sputter-etching introduces an extreme degree of structural disorder in the surface region. The LEIS pattern of such a surface is obliterated, indicating that ordered-domain sizes are less than 3 atoms in diameter, (25) there is thus at best only very-short-range order in the sputter-etched surface. The composition of the sputter-etched  $\omega\text{As}$  "surface" is 50%  $\pm 2\%$   $\omega$

valence band is p-like, peak "1" at 11 eV is s-like, and the "peak" "1" between D and E is p-like. (20) Matrix element considerations cause the s-like states to dominate the valence band spectra determined from  $M_{45V}$  transitions in these elements. (20)

When oxygen is chemisorbed on the  $\omega\text{As}(110)$  surface, the Auger lineshapes undergo changes. In order to interpret these changes, the oxygen coverage,  $\nu$ , must be known. To obtain the coverage as a function of exposure, concentrations of  $\omega$ ,  $\omega$ , and  $\text{As}$  were measured, using the 0 KVV peak height and the  $\omega$  and  $\text{As}$  1M peak heights, with the appropriate sensitivity factors. (14) Oxygen concentrations were calculated for a model of  $\nu$  sitting on top of  $\omega\text{As}(110)$ , assuming no rearrangement of  $\omega$ ,  $\omega$ , or  $\text{As}$  perpendicular to the surface and using appropriate escape depths (25) and the bulk interplanar distance of 2 Å. Measured concentrations for various oxygen exposures were then compared to these calculations to estimate the resulting oxygen coverages. Figure 2 shows the variation of oxygen coverage with exposure. The error bars are a composite of an estimate of the uncertainty in Auger peak heights due to instrumental factors and the observed variation of Auger signal in different areas on a given surface. The accuracy of the absolute coverages depends additionally, of course, on the accuracy of the electron escape depths and the relative Auger sensitivity factors in the model calculations. A  $\pm 50\%$  change in the oxygen sensitivity factor results in coverages of .7 and 1.9 monolayers at the exposure corresponding nominally to one monolayer. A  $\pm 20\%$  change in the average mean free path results in coverages of .8 and 1.3 monolayers. These uncertainties are not included in the error bars. Our coverage calculation is in general agreement with those of others. (2,9,6,8)

and 42% ± 2% As, measured using the  $\omega$  and As LMM and MVM Auger peak heights and the same sensitivity factors as for the clean cleaved surface. Because  $\omega$ As can exist as a single phase over only a very narrow composition range, 49.935 - 50.015 atomic percent  $\omega$ , (36) any  $\omega$  in excess of this range will form a second phase. This second phase appears as  $\omega$  "bubbles" that are of the order of 1  $\mu$ m in diameter or smaller, covering about 20% of the sputter-etched surface. (37) Up to a monolayer of excess  $\omega$  uniformly covering the surface cannot be excluded on the basis of the bulk phase diagram, (36) but appears to be inconsistent with the composition measurements, given the areal density of  $\omega$  "bubbles".

To illustrate the effect of sputter-etching on the local electronic properties, Fig. 4 shows a comparison of the  $M_{145}V$ -derived  $\omega$  and As-specific densities of states from clean cleaved and sputter-etched  $\omega$ As, along with the  $M_{145}V$ -derived density of states from sputter-etched elemental  $\omega$ . The major influence of sputter-etching on the  $\omega$ -specific density of states in  $\omega$ As is an increase in intensity at the top of the valence band, and an overall broadening of the lineshape due to the disorder introduced in the  $\omega$ As phase. (37) The  $\omega$  line in sputter-etched  $\omega$ As (110) can be considered as the superposition of lines for pure  $\omega$  and for  $\omega$  in stoichiometric  $\omega$ As. The As-specific density of states shows an overall broadening. The integrated intensity in the As lineshape is reduced relative to that of  $\omega$  because of the loss of As from the surface layers upon sputter-etching.

The oxygen coverage on the sputter-etched surface is plotted as a function of exposure in Fig. 5. Several points are worth noting in comparing this figure with Fig. 2. For the lowest exposures (10 l and 10<sup>3</sup> l), the resulting coverage on the initially sputter-etched surface is roughly 4 times that on the initially cleaved surface. While a coverage of approximately one

monolayer is achieved with about 10<sup>3</sup> l on the cleaved surface, one-monolayer coverage occurs on the sputter-etched surface already for exposures near 10<sup>2</sup> l.

1. There is no change in the As/ $\omega$  ratio for oxygen coverages up to this point. There is, however, a definite decrease in the As signal beyond this exposure. For an exposure of 3x10<sup>11</sup> l, there is little As left in the sample volume probed by these Auger electrons.

2. The  $M_{145}V$ -derived  $\omega$  and As-specific densities of states obtained at different oxygen coverages on the sputter-etched surface are shown in Fig. 6. There are no detectable changes in the  $\omega$ -specific density of states for coverages up to  $\theta = 0.15$ , in contrast to the results on the cleaved surface.

3. On the other hand, the features that develop in the line shape of the cleaved surface at finite  $\theta$  coverage are already present to some degree on the sputter-etched surface at zero coverage. At higher  $\theta$  coverages, the behavior is similar to that of the cleaved surface. In particular, the feature below peak C that was evident in the spectra from the cleaved surface appears above  $\theta = 0.4$  and continues to increase for larger oxygen coverages, as was the case on the cleaved surface. The major effect of changing oxygen coverage on the As spectrum for the sputter-etched surface is similar to that on the cleaved surface, i.e., a decrease in intensity at the top of the band and an increase in the middle of the band. No change is observed below  $\theta = 0.15$ . After the sputter-etched surface is exposed to 10<sup>11</sup> l, the total intensity in the As  $M_{145}V$  line is greatly reduced, and the  $\omega$  spectrum is similar to that for oxidized  $\omega$ , as shown below.

## V. DISCUSSION

In this section we summarize and compare the results of the previous two sections and discuss the implications of these results.

Oxygen adsorption on the cleaved surface causes significant changes in the U-specific density of states already at the lowest measured coverages of oxygen. The lineshape appears to change in two stages, a rather significant initial change below  $\theta = 0.1$ , and a more gentle, continuous change thereafter. The As-specific density of states changes much more subtly and apparently continuously from zero coverage up to one monolayer. The ratio of the integrated intensities in the U and As spectra increases as a function of coverage. The coverage on the cleaved surface appears to saturate at about one monolayer with a very slow increase in U concentration on the surface with increasing exposure beyond that required to form a monolayer.

Oxygen adsorption on a sputter-etched surface causes observable changes in the line shapes only for  $\theta > 0.15$ . The changes in the spectra beyond this coverage are similar to those occurring on the cleaved surface. For large exposures the sputter-etched surface shows only a weak As line, indicating the sample volume probed by the electrons that make up these Auger lines is depleted of As. The U concentration on the sputter-etched surface continues to increase beyond that required for a monolayer as the exposure is increased.

Although the Auger spectra shown in Figs. 3 and 6 do not, of course, give the species-specific density of states directly, but rather a transition density of states that depends on matrix elements and the fact that the final state is an ion, these factors should not depend on coverage, or at worst only weakly so. We therefore believe that the changes in the spectra with changing coverage can be interpreted in terms of a changing local charge density. The

total charge around each species can be considered to be proportional to the integral under the line, keeping in mind that the U/As ratio doesn't change for coverages below one monolayer. In Fig. 7 the ratio of the integrated intensities in the U and As spectra from Fig. 3 is plotted as a function of coverage. The ratio increases continuously with increasing oxygen coverage, implying an increase in electron density around U sites relative to As sites. To obtain Figs. 3 and 6 the sum of the integrals under the U and As spectra was normalized at each coverage to the zero-coverage result. This procedure determines only the relative electron density at each species. Because of the deconvolution it is not possible to relate quantitatively the integrals under spectra at different coverages to each other; hence it is not possible to say whether the increased charge at the U sites is entirely due to U electrons or whether charge transfer from As to U sites also occurs. In all likelihood, both processes affect the local charge around each species. It is not possible at this stage to separate the two effects.

The Auger line of course, gives an average over several layers. At the energies of these lines, the mean free path is such ( $\lambda$ ) that the surface layer contributes only about one fourth of the intensity. If one assumes that the charge distribution changes only in the outer layer, the increase in charge or charge transfer for the surface atom must be much larger than indicated in Figs. 3 and 6. Without the availability of absolute intensities, it is not possible to provide an explicit surface layer contribution even if the mean free path is accurately known.

Changes in the relative population of states at the U and As sites with increasing oxygen coverage can also be observed. They are, of course, inherent in Figs. 3 and 6. Figures 8 and 9 show these changes in a more direct way. To obtain Figs. 8 and 9, the areas of the U and the As spectra

were separately normalized to their respective zero-coverage values, making it straightforward to observe relative changes in population of the different states that make up the species-specific DOS. The stoichiometry does not change in the coverage range plotted in Figs. 8 and 9 (except, as indicated, for the highest exposure on the sputter-etched surface), and hence there is no contribution to the area under a line from a changing concentration of a species. This procedure should therefore suffice to determine the relative population in the different electronic states at different coverages.

Three conclusions can be drawn with the help of Figs. 8 and 9. The first is that there appear to be two regimes in O chemisorption on cleaved GaAs(110), with a dividing line at  $\theta \approx 0.1$ , in agreement with earlier work.<sup>(4,5)</sup> The second is that, above  $\theta \approx 0.1$ , the  $\omega$  line shape for oxygen-covered cleaved GaAs (110) can be fitted with a superposition of spectra for  $\omega$  in  $\omega_2\text{O}_3$  and  $\omega$  in GaAs. Figure 10 shows the  $\omega$ -specific DOS's for 1) sputter-etched elemental Ga, 2) sputter-etched  $\omega$  exposed to  $10^6$  L oxygen, 3) sputter-etched GaAs exposed to  $10^{11}$  L oxygen, 4) cleaved GaAs with about one monolayer of oxygen adsorbed on it, and 5) clean cleaved GaAs. Spectrum 2) is representative of oxide on  $\omega$ ; from thermodynamic considerations, this oxide is expected to be  $\omega_2\text{O}_3$ .<sup>(18)</sup> The most notable feature in spectrum 2) is a peak at  $-9.5$  eV; this peak is also the one that grows in the other spectra upon O chemisorption. Figure 11 shows a fit of the  $\omega$  spectrum with a superposition of  $\omega$  lines from  $\omega_2\text{O}_3$  and GaAs. It appears that the electronic charge distribution around  $\omega$  for O chemisorbed on the cleaved GaAs surface is similar to that of bulk  $\omega_2\text{O}_3$ .

The third conclusion that can be drawn is that the Ga and As spectra for both initial surface conditions become similar for coverages above about 1/2 monolayer, even though the exposures required to get to these coverages are

quite different for the two surface conditions. This implies that the local surface chemical arrangement is the same in both surfaces, which can be understood in the following way. On the sputter-etched surface two chemisorption processes compete: adsorption onto the Ga bubbles and attack of Ga and As bonds in the disordered GaAs. It is presumably easier to chemisorb O on the Ga bubbles and thus this process occurs preferentially. The types of bonds that are formed on Ga and on GaAs (both cleaved and sputter-etched) must be very similar, i.e., the Ga atoms must be strongly involved and the "surface compound" that is formed must look like a Ga oxide. If this were not the case, i.e. if the bonding of O on Ga were different from that on GaAs, the differences in the clean-surface spectra would continue to manifest themselves for all coverages.

It is interesting to speculate at this point why the bonding on the cleaved and sputter-etched surfaces should be similar. A model consistent with this fact is that oxygen chemisorption is essentially a defect-related mechanism.<sup>(4-7,9)</sup> Chemisorption is then initiated at structural defects. The bonding itself creates a disordered surface, i.e., one that consists of structural defects. On the sputter-etched surfaces the concentration of initial defects is much higher, and thus a higher chemisorption rate results. It is probable that atomic oxygen is inserted into Ga and As back bonds. The insertion of oxygen into back bonds on the cleaved surface may initially be restricted to atom defect sites and subsequently to surface layer atoms in the vicinity of these defects. This would imply that regions of disorder caused by O chemisorption nucleate at structural defects and grow outward from them, leaving the surface looking essentially like "swiss cheese", with regions of surface disorder surrounded by "good" GaAs surface. This model of the surface structure can in principle be checked by LEIS

angular profile analysis.(39) The regions of disorder will produce only diffuse intensity, but, because they are arranged in patches, they will remove intensity from the diffracted beams in a characteristic way that depends on the size distribution and arrangement of those patches. The resulting diffracted beam line shape then directly reflects this distribution.(40) Although visual observations of LEIS beams have been made,(8) we are not aware of any attempts to measure actual diffracted-beam shapes for this system.

The increase in oxygen concentration above one monolayer with increasing exposure on the sputter-etched surface can also be explained on the basis of defects. The sputter-etched surface has such a high degree of disorder, and a resulting high density of broken bonds, that oxygen can probably attack to a depth of many average layer distances, allowing "bulk" oxidation to take place readily without a significant "structural" activation barrier. This bulk oxidation is evidenced by the  $\omega$ As spectrum for high U exposures and the depletion of As in the surface region, as was shown in fig. 6. It is apparent that a  $\omega$ As oxide has formed.

We now comment briefly on possible models for the equilibrium position of oxygen atoms chemisorbed on the  $\omega$ As surface. As already mentioned, there are several of these.(2,4,5,13) because of the possibility of charge transfer between Ga and As, it is impossible to say anything definitive about the equilibrium site without the help of calculations. However, physically reasonable models can be postulated with the assumption that this charge transfer is small. For  $u > 0.1$  it appears that both  $\omega$ -U and As-U bonds form. The  $\omega$ -U bonding at all coverages above  $u = 0.1$  appears to be similar to that in  $\omega_2O_3$ . Because we do not have access to a variety of Ga oxides, it is not possible to say whether different Ga oxides will produce different Auger line shapes. Hence the determination of similarity to  $\omega_2O_3$  is not

unique. We do not believe that the feature in the oxidized- $\omega$ As spectrum is due to the oxygen atom. AES is a local probe, but one could imagine the O atom sitting close enough to the Ga atoms for U wave function overlap to occur onto the Ga core. However, U does not have a spectral feature at -9.5 eV.(4) Also, if the U feature were observed in the  $\omega$ As spectrum it should, in all likelihood, also be observed in the As spectrum, unless the U atoms were significantly closer to the Ga atoms. It also appears that the mechanism for oxygen bonding does not change above  $u = 0.1$ . We arrive at this conclusion in the following way. In Fig. 11 a fit to the  $\omega$ As line for  $\omega$ As with various coverages of U was shown. The area under the "oxide" contribution to the spectrum can be considered as the oxygen "coverage" on the Ga sites. If the change in this area is compared to the total U coverage, it is found that the two scale. Hence there can be no change in the bonding geometry (at least for  $u \geq 0.1$ ) that would produce a significant difference in charge distribution. It is not, for example, possible for bonding to occur initially on Ga sites and later on As sites.

The model of Iudate,(2) consisting of oxygen bridge bonds to surface Ga and As atoms, most closely matches the constraints imposed by our data (with the assumption of negligible charge transfer between Ga and As). Simpler models do not appear to be satisfactory. We have made attempts to match our spectra with layer-averaged charge densities produced in calculations for simple models(17) but have not found it possible to draw a correspondence in the trends of the experimental and theoretical spectra.

There is, of course, the possibility that charge transfer plays the major role in the species-specific change density. Calculations(17) of the density of states in the surface layer of GaAs with U adsorbed in either the Ga or As show a large increase in the density of states at the bottom of

the  $\text{LaAs}$  valence band if U adsorbs on As, but a much smaller change if U adsorbs on La. We do observe a change at the bottom of the valence band, but only for the La-specific density of states. At first glance one would draw the conclusion that U bonds to As and that charge is transferred back to La. Whereas this may be the case, the conclusion can not be drawn unequivocally without projecting the densities of states in the calculations onto the La and As atoms separately, because both La and As have states at the bottom of the valence band. (20) Furthermore calculations are required for a variety of other sites to affirm this conclusion.

The coverage regime below  $u < 0.1$  appears to be different from that for  $u > 0.1$ . Below this coverage there appear to be no effects on the La or As core levels and no visible oxygen derived features in the UPS valence band spectrum. (4) There are however, effects on surface states and on Fermi level pinning. (4) Band bending due to poor cleavage quality has also been reported. (1,2) Crystalline defects such as steps or point defects can play a similar role in pinning the Fermi level. We believe that the changes observed in the La line shapes at coverage, as low as  $u = 0.04$  give evidence that changes in the charge density around La are in some manner associated with Fermi level pinning. Changes similar to those observed in the La line at low U coverage are also observed in LaAs that has been lightly sputter etched or not fully annealed, as well as for surfaces that have been poorly cleaved. Fermi level pinning has been observed to occur in these situations. (1,2) We conclude that it is the La atoms, in all likelihood occurring at structural defect sites, that undergo the charge distribution changes necessary to pin the Fermi level. Adsorption occurs preferentially at these defect sites. However, we envision the chemisorption of U on LaAs not as a strictly sequential process, but rather as a competition between two

simultaneously occurring processes that have different activation energies. There are the adsorption at defect sites, which we believe to be La sites, and adsorption onto LaAs terraces, which we believe "spreads out" from such defect sites, growing more or less two-dimensionally into patches of disordered surface "oxide" involving both La and As atoms.

#### V. CONCLUSIONS

We have reported measurements of changes in the species-specific densities of filled states in the chemisorption of oxygen on LaAs(110), by using Auger line shapes of transitions that involve the valence band. We have demonstrated that a fingerprint of the charge density around individual species in a multicomponent system can be obtained as a function of coverage by measuring these line shapes. There are, of course, difficulties with an absolute interpretation of such a line shape, as there is with all electron spectroscopic measurements. For one, the matrix elements for the transitions are in general not accurately known. Second, the final state in the Auger process is an ion, and thus the measurement does not represent the ground state charge density. Third, relaxation effects may be important. They should be much less of a problem in LaAs than for materials with sharply peaked densities of states, such as d-band metals. None of these factors should significantly affect the changes in the spectra with coverage, and hence we believe that these changes can be directly interpreted as changes in the local charge configuration. As we have already discussed, there is additionally the difficulty (again inherent in all surface spectroscopies) that the measurement represents an average over several layers.

We have interpreted the line shapes in the simple limit of zero charge transfer between La and As atoms with increasing U coverage. This may not be reasonable, but in the absence of calculations, one cannot conclude that it is

not. We hope that our measurements will stimulate further theoretical work on the subject. We believe that a correlation of structural defects with measurements of localized electronic properties such as these will provide information on Fermi level pinning and Schottky barriers. Analysis of surface structural defects, even at quite low concentrations, is possible using LEIS or HREIS. We are presently combining these techniques with Auger line shape analysis to investigate more fully the relationship between structural defects, Fermi level pinning, and the initial stages of chemisorption in this surface.

#### Acknowledgements

We thank D. E. Savage and H. M. Clearfield for useful discussions.

#### References

1. M. Laitat and D. I. Eastman, *J. Vac. Sci. Technol.* **13**, B31 (1976).
2. K. Luikko, *Solid State Comm.* **21**, 815 (1977).
3. H. Luth, M. Buchel, K. Horn, M. Ueier, and R. Matz, *Phys. Rev.* **B15**, 865 (1977).
4. C. R. Brundle and D. Seybold, *J. Vac. Sci. Technol.* **16**, 1186 (1979).
5. C. Y. Su, I. Lindau, P. K. Skeath, P. W. Chye, and M. E. Spicer, *J. Vac. Sci. Technol.* **17**, 936 (1980).
6. P. W. Chye, C. Y. Su, I. Lindau, P. K. Skeath, and M. E. Spicer, *J. Vac. Sci. Technol.* **16**, 1191 (1979).
7. J. Stohr, R. S. Bauer, J. C. McManis, I. I. Johansson, and S. Brennan, *J. Vac. Sci. Technol.* **16**, 1195 (1979).
8. A. Kahn, D. Kanani, P. Mark, P. W. Chye, C. Y. Su, I. Lindau, and M. E. Spicer, *Surface Sci.* **87**, 375 (1979); A. Kahn, D. Kanani, and P. Mark, *Surface Sci.* **94**, 545 (1980).
9. P. Mark, E. So, and M. Bonn, *J. Vac. Sci. Technol.* **14**, 865 (1977).
10. J. J. Barton, M. A. Gaddard, III, and T. C. McGill, *J. Vac. Sci. Technol.* **16**, 1178 (1979).
11. P. Pianetta, I. Lindau, C. M. Garner, and M. E. Spicer, *Phys. Rev.* **B18**, 2792 (1978).
12. P. Mark and M. E. Creighton, *Thin Solid Films* **56**, 19 (1979).
13. G. Lucovsky, *J. Vac. Sci. Technol.* **19**, 456 (1981).
14. J. J. Barton, C. A. Swarts, M. A. Gaddard III, and T. C. McGill, *J. Vac. Sci. Technol.* **17**, 164 (1980).

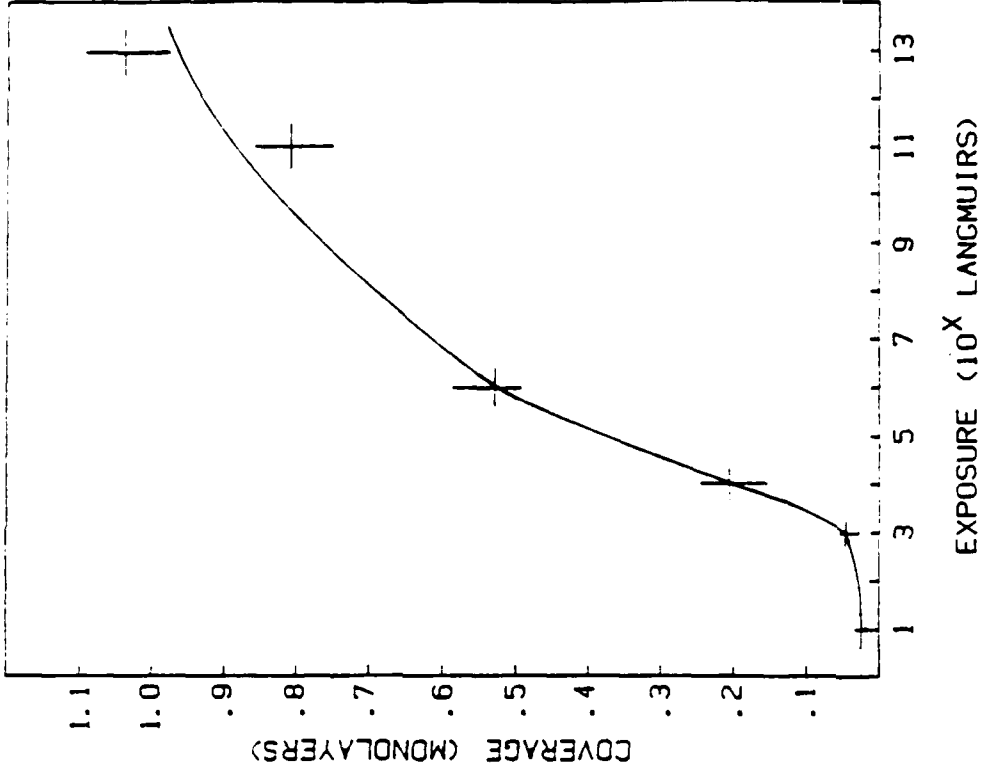
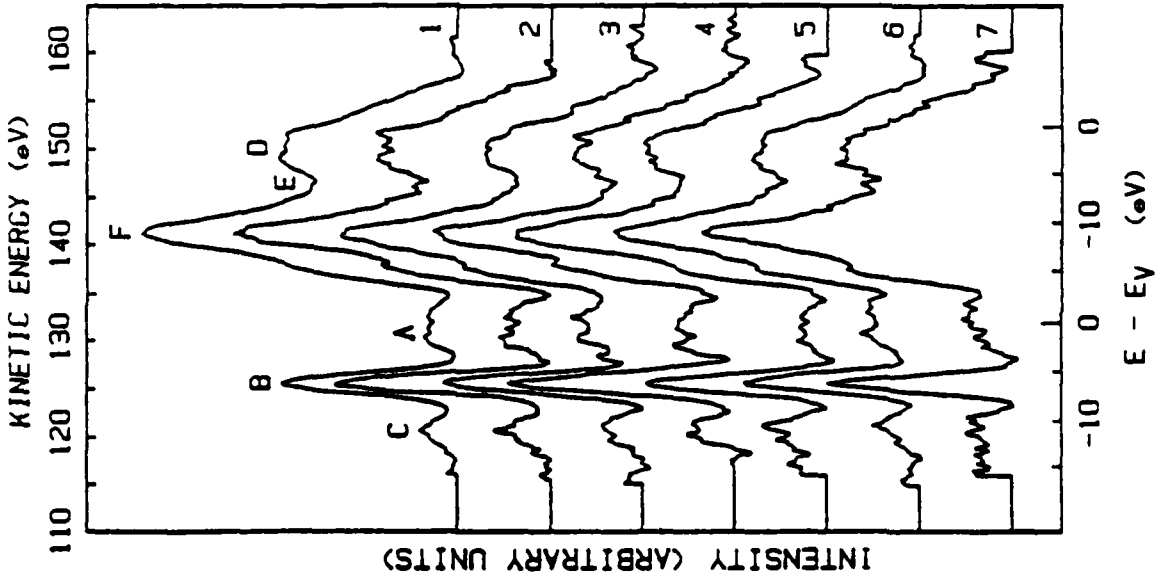
15. M. A. Laddard, III, J. Barton, A. Reibomb, and I. L. McGill, *J. Vac. Sci. Technol.*, **15**, 1274 (1978).
16. M. Munch and R. Enninghurst, *J. Vac. Sci. Technol.*, **17**, 942 (1980).
17. E. J. Mele and J. D. Joannopoulos, *Phys. Rev. B*, **18**, 6999 (1978).
18. R. Ludeke, *Phys. Rev. B*, **16**, 5598 (1977).
19. V. Heine, *Phys. Rev.*, **151**, 561 (1966).
20. P. J. Fetteleman, L. J. McGuire, and K. C. Pandey, *Phys. Rev. B*, **16**, 5499 (1977).
21. G. D. Davis and M. G. Lagally, *J. Vac. Sci. Technol.*, **15**, 1311 (1978).
22. J. Tejeda, M. Cardona, M. J. Shevchik, D. M. Langer, and E. Schonherr, *Phys. Stat. Sol.*, **B58**, 189 (1973).
23. J. Tejeda, M. J. Shevchik, D. M. Langer, and M. Cardona, *Phys. Rev. Lett.*, **30**, 370 (1973); J. L. Fuggle, L. M. Watson, P. R. Morris, and D. J. Fabian, *J. Phys. F*, **5**, 590 (1975).
24. H. M. Clearfield, M. G. Lagally, *J. Vac. Sci. Technol.*, submitted.
25. K. D. Childs and M. G. Lagally, in preparation.
26. M. M. Mularie and M. I. Perla, *Surface Sci.*, **26**, 125 (1971).
27. J. L. Houston, *J. Vac. Sci. Technol.*, **12**, 255 (1975).
28. H. H. Madden and J. E. Houston, *J. Appl. Phys.*, **47**, 3071 (1976).
29. P. H. Van Cittert, *Z. Phys.*, **69**, 304 (1931).
30. G. D. Davis, P. E. Viljoen, and M. G. Lagally, *J. Electron Spectrosc. Relat. Phenom.*, **20**, 305 (1980).
31. G. D. Davis, P. E. Viljoen, and M. G. Lagally, *J. Electron Spectrosc. Relat. Phenom.*, **21**, 135 (1980).
32. K. D. Childs and M. G. Lagally, *J. Vac. Sci. Technol.*, submitted.
33. The relative sensitivity factors for Ga and As were obtained from clean cleaved GaAs, and that for D is from the Handbook of Auger Electron Spectroscopy, Physical Electronics Industries (1975).
34. H. Lant and M. Munch, *Surface Sci.*, **105**, 217 (1981).
35. M. Hansen and K. Aulterko, *Constitution of Binary Alloys*, McGraw-Hill, New York, 1958.
36. G. D. Davis, D. L. Savage, and M. G. Lagally, *J. Electron Spectrosc. Relat. Phenom.*, **23**, 25 (1981).
37. D. Kubaschewski and C. B. Alcock, *Metallurgical Thermodynamics*, 5th ed., Pergamon, Oxford (1973).
38. D. L. Savage, D. Saloner, and M. G. Lagally, in preparation.
39. A. Gantner, *X-Ray Diffraction*, M. H. Freeman Co., San Francisco, CA (1963).

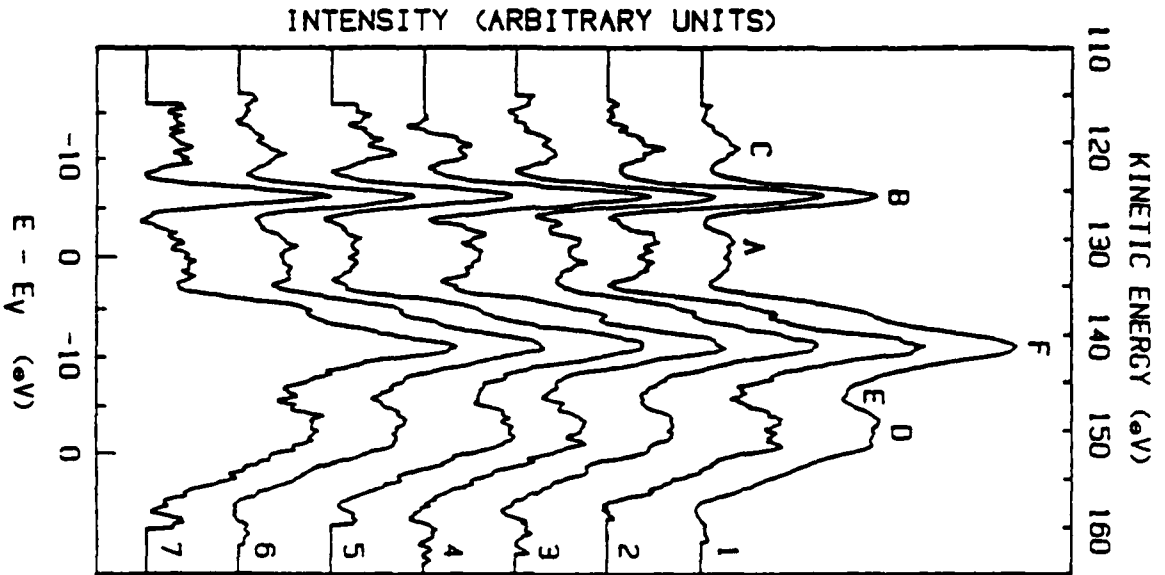


## Figure Captions

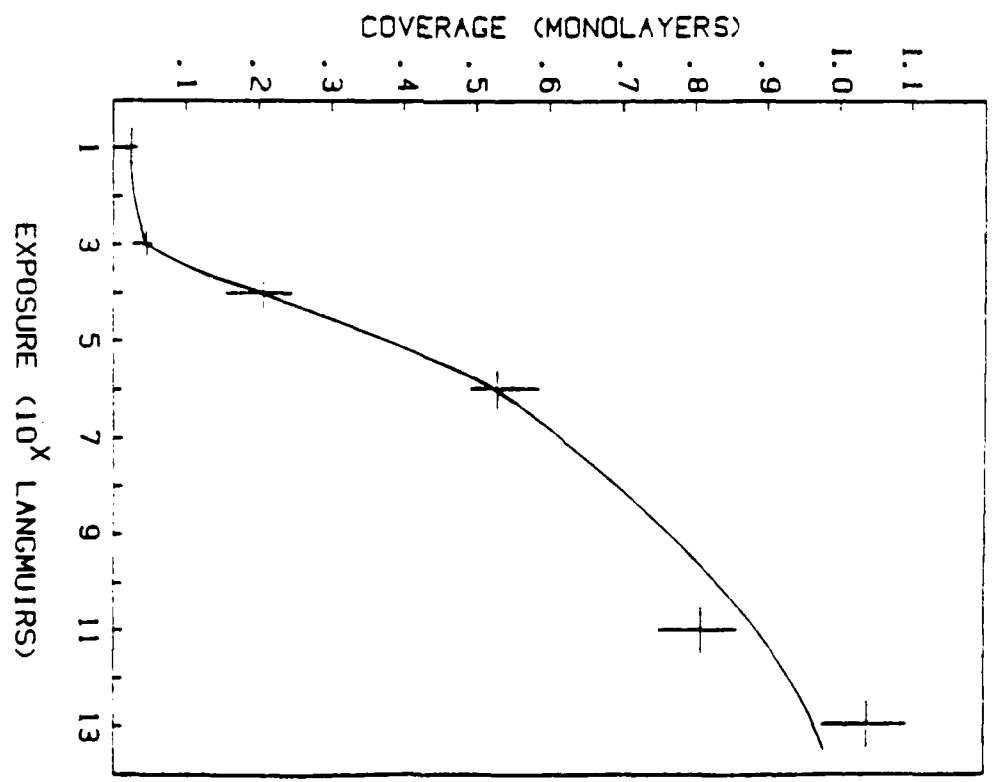
- Fig. 1 Ga and As species-specific densities of states for clean cleaved GaAs(110) derived from  $M_1M_{2,3}V$  Auger lines. The Ga spectrum lies between 115 and 135 eV, and the As spectrum between 135 and 160 eV. Curves 1 and 2: Results for 2 extreme conditions in the deconvolution procedure. Curves 2 through 6: Four different cleaves and two locations on one cleavage face. Curve 7: Spectrum using 1 eV modulation. The bottom scale was determined by rigidly aligning the spectra with corresponding peaks in the XPS valence band spectrum.
- Fig. 2 Oxygen coverage on cleaved GaAs(110) as a function of exposure.
- Fig. 3 Ga and As species-specific densities of states for different oxygen coverages on cleaved GaAs(110). The total area under each curve is normalized to that of the clean surface. The oxygen coverage is listed in fractions of a monolayer.
- Fig. 4 Ga and As species-specific densities of states for 1) sputter-etched GaAs(110) and 2) cleaved GaAs(110), and 3) the Ga-specific density of states for elemental Ga.
- Fig. 5 Oxygen coverage on sputter-etched GaAs(110) as a function of exposure.
- Fig. 6 Ga and As species-specific densities of states for different oxygen coverages on sputter-etched GaAs(110). The total area under each curve is normalized to that of the clean surface. The oxygen coverage is listed in fractions of a monolayer. The top spectrum results from an exposure of  $10^{13}$  l. It shows a very strong Ga line and depletion of As.

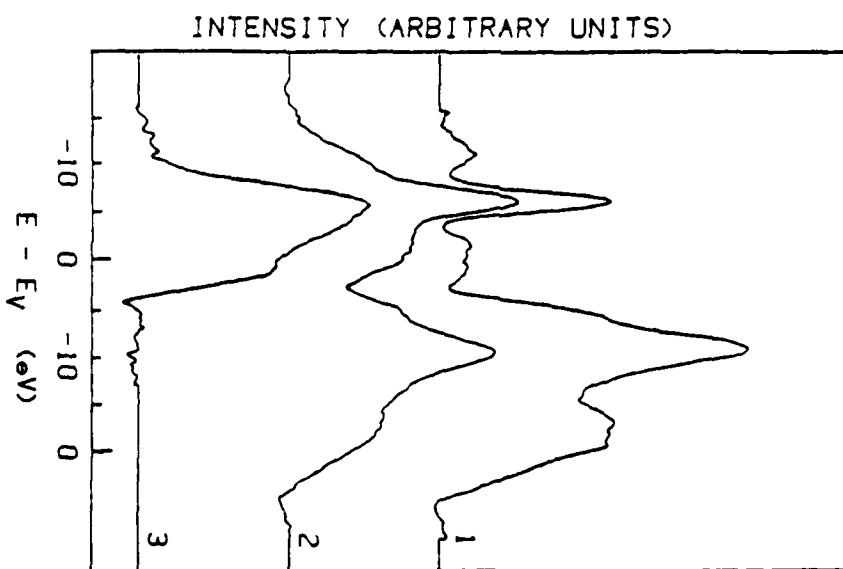
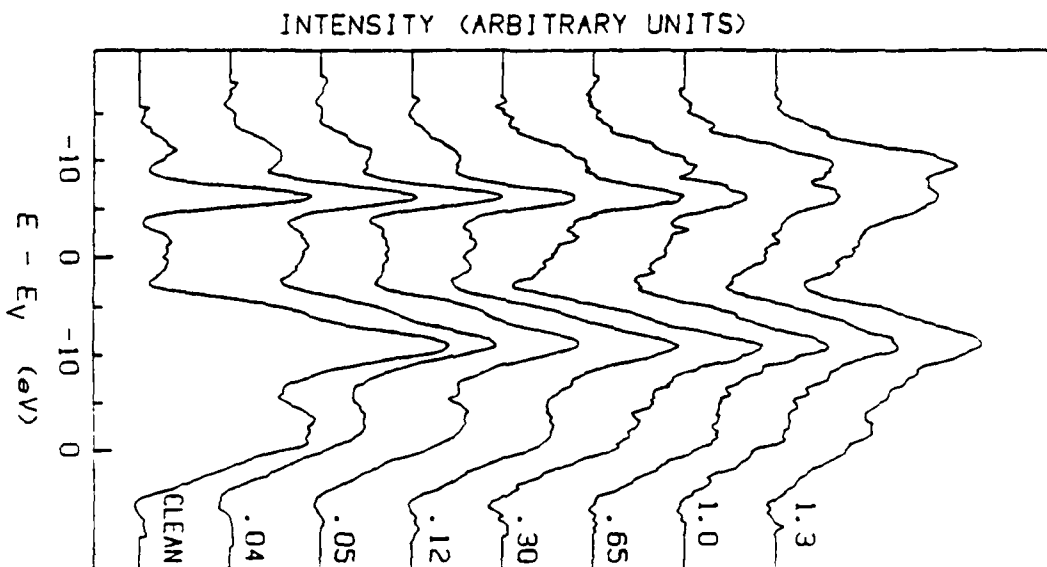
- Fig. 7 The ratio of the integrated intensities in the Ga-specific and As-specific densities of states as a function of oxygen coverage on the cleaved surface.
- Fig. 8 Distribution of states within the species-specific densities of states for different oxygen coverages on cleaved GaAs(110). a) Ga, b) As. The Ga and As spectra are separately normalized to constant areas. The Ga/As ratio remains constant for all coverages. The values are coverages in monolayers.
- Fig. 9 Distribution of states within the species-specific densities of states for different oxygen coverages on sputter-etched GaAs(110). The Ga and As spectra are separately normalized to constant areas. The Ga/As ratio remains constant, except for the top spectrum, which can thus not be compared directly to the others.
- Fig. 10 The Ga-specific density of states for 1) clean elemental Ga, 2) oxidized elemental Ga, 3) sputter-etched GaAs(110) exposed to  $10^{14}$  oxygen, 4) one monolayer of oxygen adsorbed on cleaved GaAs(110), and 5) clean cleaved GaAs(110).
- Fig. 11 Fits to the Ga-specific density of states for different oxygen coverages on cleaved GaAs(110) from Fig. 10, made by summing the Ga spectra for clean GaAs(110) and for oxidized Ga. Curve 1 is oxidized elemental Ga; Curves 2 through 6: fits for  $\theta = 1.3, 0.65, 0.3,$  and  $0.1$  respectively; Curve 7: clean cleaved GaAs(110).

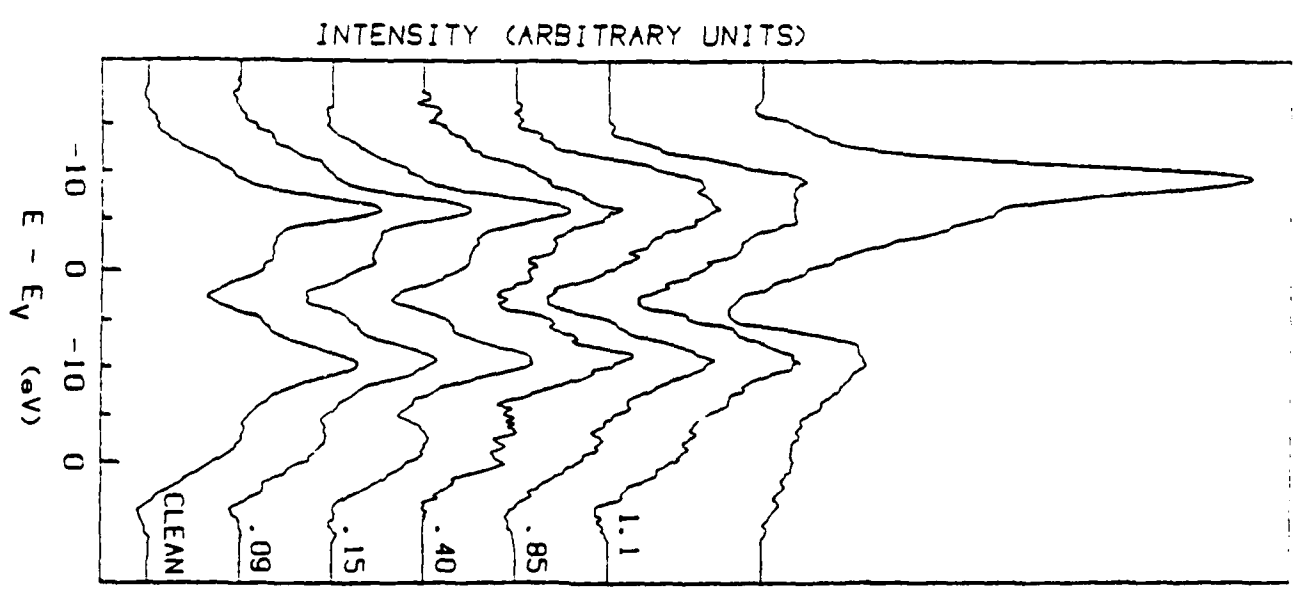
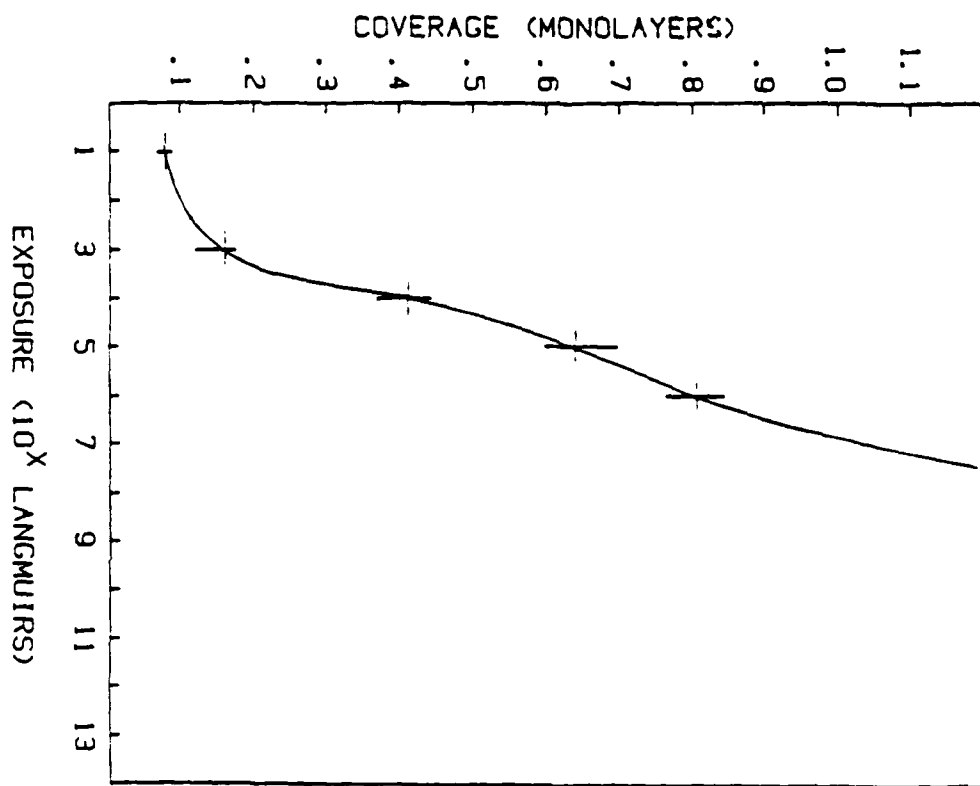


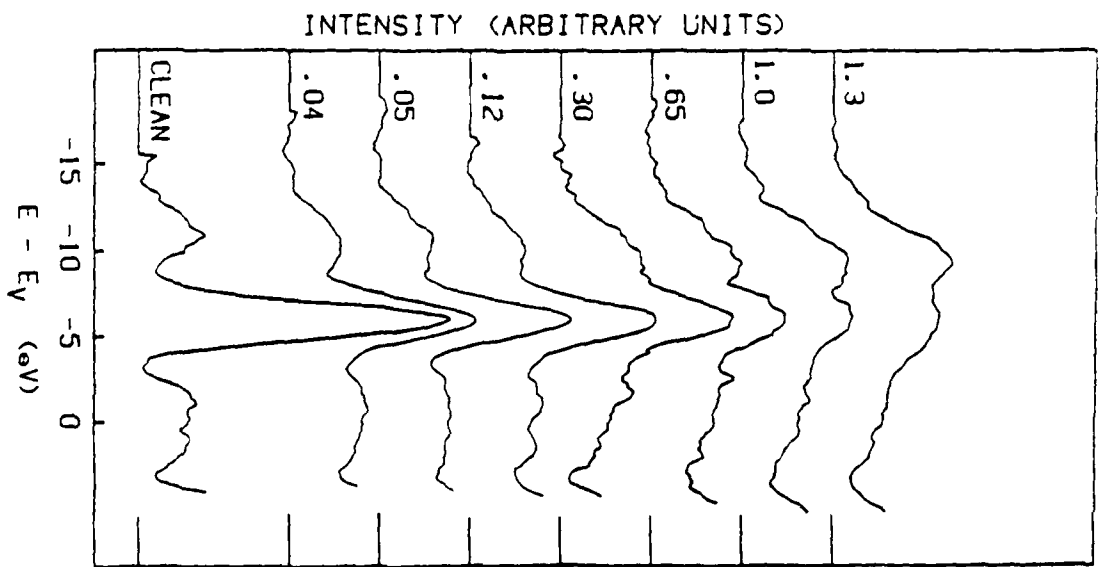
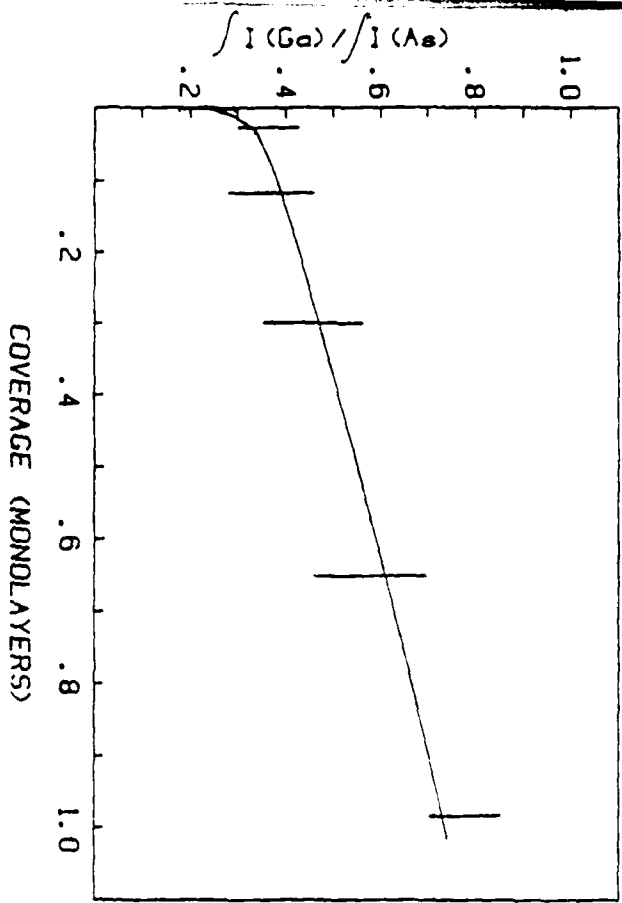


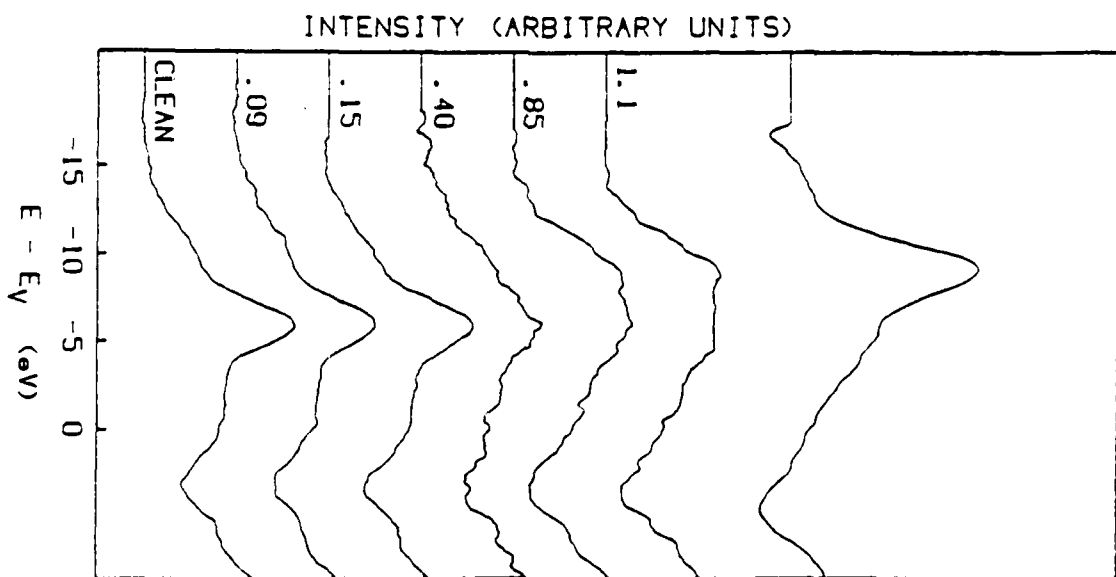
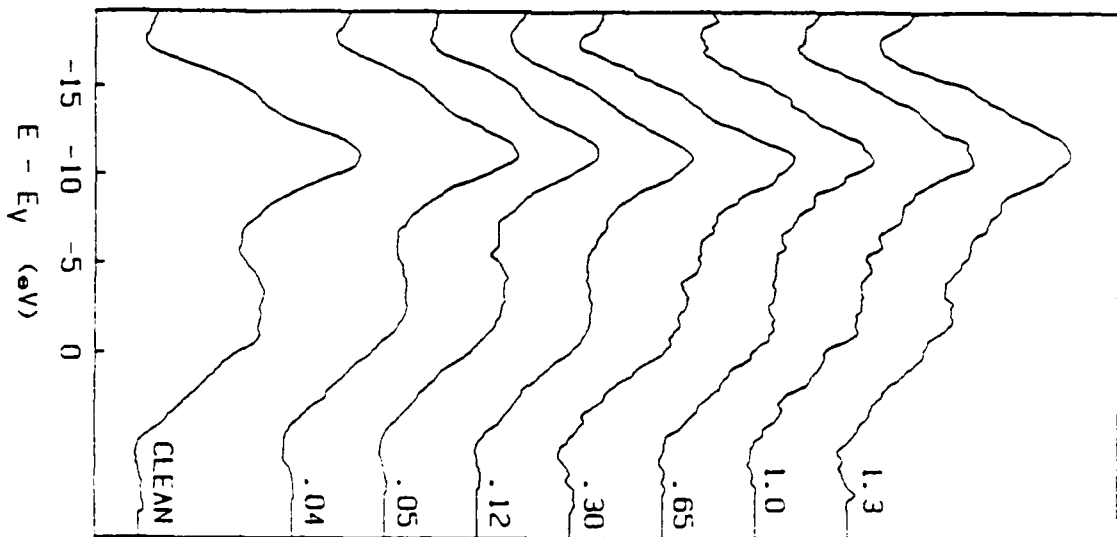
1.41

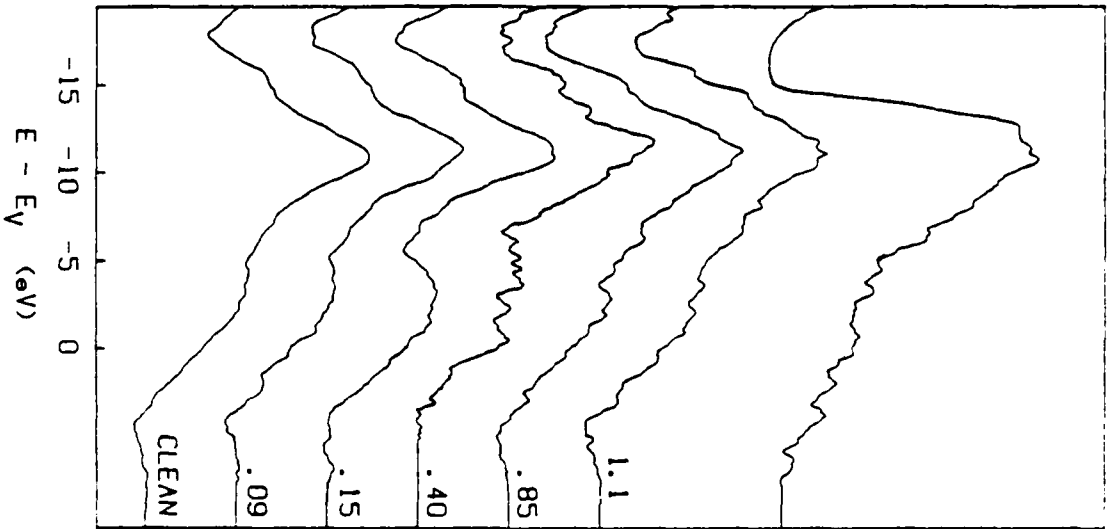




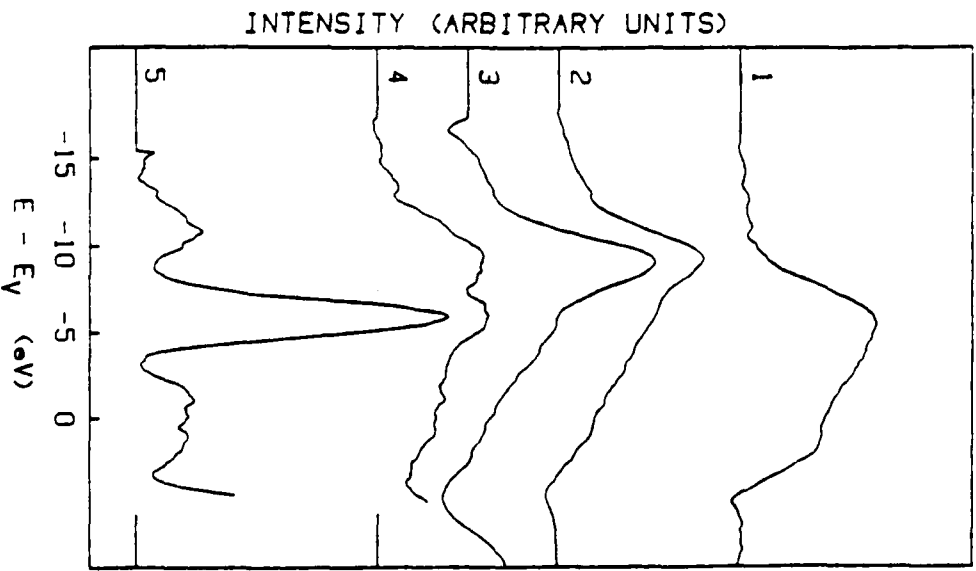




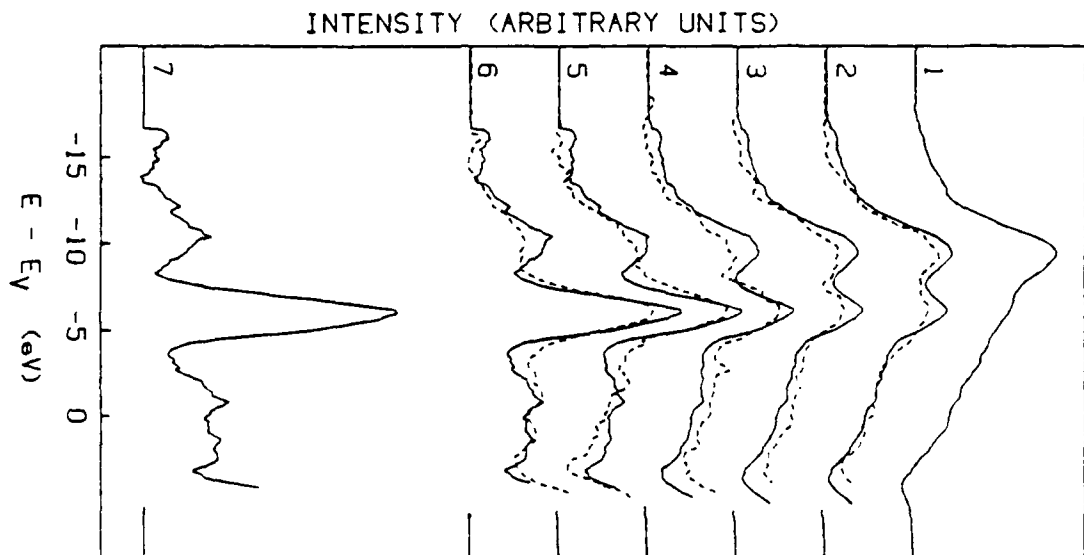




1.1







END

DATE  
FILMED

11 - 83

DTIC